





Article

Investigating the Impact of Carbon Fiber as a Wheelchair Frame Material on Its Ability to Dissipate Kinetic Energy and Reduce Vibrations

Bartosz Wieczorek ¹, Łukasz Warguła ^{1,*}, Jarosław Adamiec ¹, Tomasz Sowa ², Michał Padjasek ³,
Łukasz Padjasek ³ and Maciej Sydor ⁴

¹ Faculty of Mechanical Engineering, Institute of Machine Design, Poznan University of Technology, Piotrowo 3, 60-965 Poznań, Poland; bartosz.wieczorek@put.poznan.pl (B.W.); jaroslaw.adamiec@put.poznan.pl (J.A.)

² Scientific and Research Centre for Fire Protection, National Research Institute, Nadwiślańska 213, 05-420 Józefów, Poland; tsowa@cnbop.pl

³ Cosmotech LLC, Szyby Rycerskie 22k St., 41-909 Bytom, Poland; mp@cosmotech-3d.com (M.P.); lp@cosmotech-3d.com (Ł.P.)

⁴ Department of Woodworking and Fundamentals of Machine Design, Faculty of Forestry and Wood Technology, Poznań University of Life Sciences, 60-637 Poznań, Poland; maciej.sydor@up.poznan.pl

* Correspondence: lukasz.wargula@put.poznan.pl

Abstract: Using a wheelchair over uneven terrain generates vibrations of the human body. These vibrations result from mechanical energy impulses transferred from the ground through the wheelchair components to the user's body, which may negatively affect the quality of the wheelchair use and the user's health. This energy can be dissipated through the structure of the wheelchair frame, such as polymer and carbon fiber composites. This article aims to compare a wheelchair with an aluminum alloy frame and a carbon fiber frame in terms of reducing kinematic excitation acting on the user's body. Three wheelchairs were used in the study, one with an aluminum alloy frame (reference) and two innovative ones with composite frames. The user was sitting in the tested wheelchairs and had an accelerometer attached to their forehead. The vibrations were generated by applying impulses to the rear wheels of the wheelchair. The obtained results were analyzed and compared, especially regarding differences in the damping decrement. The research shows that using modern materials in the wheelchair frame has a beneficial effect on vibration damping. Although the frame structure and material did not significantly impact the reduction in the acceleration vector, the material and geometry had a beneficial effect on the short dissipation time of the mechanical energy generated by the kinematic excitation. Research has shown that modern construction materials, especially carbon fiber-reinforced composites, may be an alternative to traditional wheelchair suspension modules, effectively damping vibrations.

Keywords: vibration damping; vibrations; damping decrement; vibration transmission; impact on the human body



Citation: Wieczorek, B.; Warguła, Ł.; Adamiec, J.; Sowa, T.; Padjasek, M.; Padjasek, Ł.; Sydor, M. Investigating the Impact of Carbon Fiber as a Wheelchair Frame Material on Its Ability to Dissipate Kinetic Energy and Reduce Vibrations. *Materials* **2024**, *17*, 641. <https://doi.org/10.3390/ma17030641>

Academic Editor: Stefano Bellucci

Received: 21 December 2023

Revised: 23 January 2024

Accepted: 24 January 2024

Published: 29 January 2024



Copyright: © 2024 by the authors. Licensee MDPI, Basel, Switzerland. This article is an open access article distributed under the terms and conditions of the Creative Commons Attribution (CC BY) license (<https://creativecommons.org/licenses/by/4.0/>).

1. Introduction

A person using a wheelchair forms an anthropotechnical system that can be modeled with many related biomechanical and mechanical parameters and causal effects [1–3]. One such parameter relation is the movement of the human body combined with the movement of a wheelchair [4,5]. This connection results from the cyclical propelling of the wheelchair using the upper limbs and the transfer of mechanical energy to the human body through the body support system of the moving wheelchair [6]. Negotiating uneven terrain can introduce additional vertical accelerations into the wheelchair–user system, particularly when the wheelchair abruptly transitions between different height levels, such as rolling off a curb [7–9]. These abrupt changes can generate unfavorable vibrations that

significantly impact the user's comfort and stability. The source of these vibrations are stochastic impulses of mechanical energy transmitted from the ground to the human body via the wheels, frame, and seat of the wheelchair. These impulses cause short-term and sudden accelerations affecting the body and internal organs [10,11].

Human body vibrations are an unfavorable phenomenon that deteriorates the quality of wheelchair use and poses a risk to its user's health [12–15]. Therefore, the need to achieve the ability to dampen wheelchair vibrations that occur during driving is justified. The current state of technology allows for solving this problem with additional wheelchair equipment. Known solutions include shock-absorbing cushions [16–18] and shock-absorbing wheelchair suspension [19–21]. A new trend is using innovative geometric features of the wheelchair frame structure [22] or new materials that absorb vibration energy [18]. An example of a new material used in the construction of wheelchair frames is polymer and carbon fiber composites. So far, this material has been used due to a significant reduction in the weight of the wheelchair [23–25] while maintaining high stiffness, as well as due to its modern visual design.

Analyzing the available research works, there is a noticeable lack of studies analyzing the impact of carbon fiber composites in a wheelchair frame structure on the reduction in vibrations transmitted to the human body. Therefore, this study seeks to compare the shock-absorbing capabilities of a wheelchair with an aluminum alloy frame and one with a carbon fiber frame, focusing on reducing the magnitude and duration of accelerations experienced by the wheelchair user's body.




Achieving this goal required the preparation of a consistent vibration generator and the analysis of the acceleration values acting on the head of the wheelchair user and the time needed to reduce these accelerations to the level of 1 g (approximately 9.81 m/s^2). Based on the tests performed, it is possible to determine the ability of new-generation wheelchairs to dampen mechanical energy caused by kinematic excitation coming from the ground.

2. Materials and Methods

2.1. Tested Wheelchairs

We used three ultra-lightweight rigid manual self-propelled wheelchairs, one with an aluminum frame and two with a carbon fiber frame. Table 1 summarizes the tested wheelchairs: WA denotes a wheelchair with an aluminum frame, WCBK signifies a model with a carbon fiber frame and a standard seat, while WCK represents a configuration featuring a carbon fiber frame and a bucket seat.

Table 1. Morphological matrix of the tested wheelchair variants.

Variant Denotation	WA	WCK	WCBK
			
Driving wheel	pneumatic, 36 spokes, pressure 5 bar, diameter 24"	pneumatic, 36 spokes, pressure 5 bar, diameter 24"	pneumatic, 36 spokes, pressure 5 bar, diameter 24"
Caster wheel	full, diameter 4"	full, diameter 4"	full, diameter 4"
Seat cushion	pneumatic—Prevent Classic (AR-093)	pneumatic—Prevent Classic (AR-093)	pneumatic—Prevent Classic (AR-093)
Frame material	aluminum frame	carbon fiber frame	carbon fiber frame
Seat design	classic on stripes	bucket	classic on stripes
Overall mass	11.6 kg	8.2 kg	7.8 kg
Model; manufacturer	Aviator; MTB Poland, Łódź, Poland	Freeeasy Bucket; Cosmotech LLC, Bytom, Poland	Freeeasy Classic; Cosmotech LLC, Bytom, Poland

The WA, WCK, and WCBK wheelchair variants built for this study had the same running gear (drive wheels and caster wheels) and identical anti-decubitus foam cushions. The differences between the commonly used WA wheelchair with an aluminum frame and new carbon fiber (WCK and WCBK) structures resulted from the frame's material, cross-sections, and seat type (Figure 1).

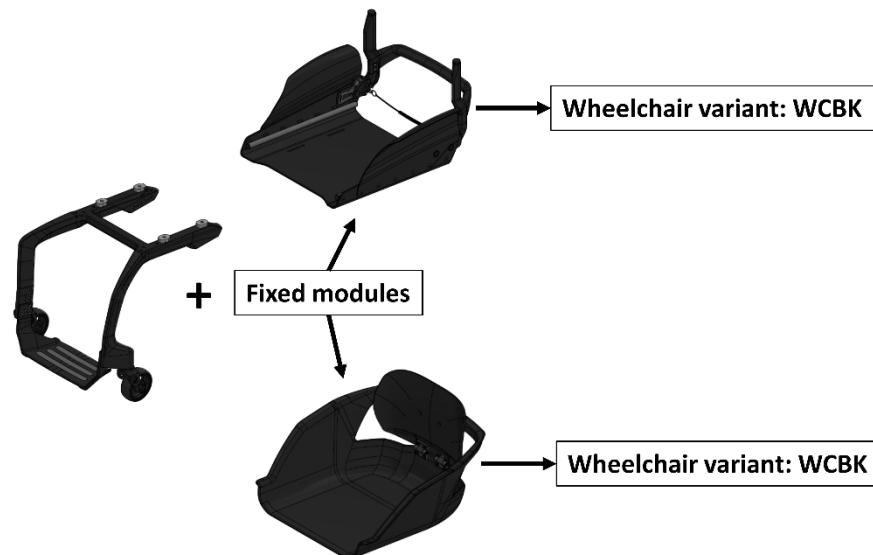


Figure 1. Configuration diagram of the Cosmotech Freeeasy classic (WCBK) and Cosmotech Freeeasy bucked (WCK) carbon fiber wheelchair modules.

During the tests, the same person was always sitting in a wheelchair: a man with a height of 176 cm and a body weight of 64 kg (the person sat motionless in an upright position). An external generator generated the vibrations. The wheelchairs were stabilized during the tests and did not move.

2.2. Research Equipment

The research was carried out using the measurement system shown in Figure 2, consisting of the tested wheelchair (1), whose front self-adjusting wheels were supported on a stationary surface (2), while the rear wheels were based on a cylinder (3) with a diameter equal to the diameter of the wheelchair's drive wheel (600 mm). The cylinder (3) was coupled to the wheel by an electric motor generating a constant rotational speed of 20 rpm, which translated into a simulated linear speed of the wheelchair of approximately 2.28 km/h. A transverse irregularity (4) with a height of 15 mm was placed on the cylinder (3), which was a generator of vibrations transmitted to the tested human wheelchair anthropotechnical system. The amplitude of each generated vibration pulse was 15 mm, and the pulse acceleration was 5.36 g.

The element recording vibrations (in the form of R acceleration) was an accelerometer (6) mounted on the person's head, attached with elastic bands, pressed to the Vertex capitis head, and stabilized in this position. The accelerometer used consisted of a KIONIX kx023 inertial sensor (with a resolution of 0.009576801 m/s² and a measurement range from 0 to 78.4532 m/s²), a data archiving system, and a power supply. The mass of the vibration recorder did not exceed 100 g, so it was insignificant compared to the overall weight of the anthropotechnical systems evaluated. The layer adapting the flat surface of the bottom of the accelerometer to the curved surface of the head of a person sitting in the tested wheelchair was made of rubber with a hardness of 40–50 according to the Shore A scale. This method of mounting the vibration recorder is consistent with the guidelines contained in the PN-EN ISO standard 5349-1:2004 [26] for the supporting frame to which the drive unit and supports holding the entire device on the ground were also attached. The position

of the accelerometer's X, Y, and Z measurement axes relative to the frame of the tested wheelchairs is shown in Figure 2.

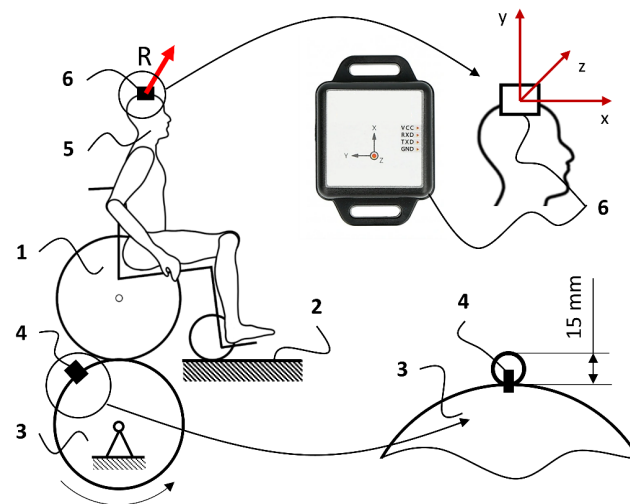


Figure 2. Diagram of the measurement system used, where 1—tested wheelchair, 2—stationary surface stabilizing the wheelchair, 3—cylinder supporting and propelling the rear wheels of the wheelchair, 4—transverse inequality generating kinematic excitation, 5—human exposed to vibrations, 6—accelerometer.

2.3. Analytical Model

The analytical model of the studied system, with an indication of the analyzed element in terms of energy dissipation properties, is depicted in Figure 3. This model divides the studied system into components: front wheel, rear wheel, wheelchair frame, human body, and head. Such a segmented division of the system and the connections between segments are consistent with scientific works dedicated to modeling the vibrations of a wheelchair. The last segment, the head, provided the measured signal during the study, which was the subject of the analysis of the influence of the frame material on the dissipation of acceleration transferred to the human body.

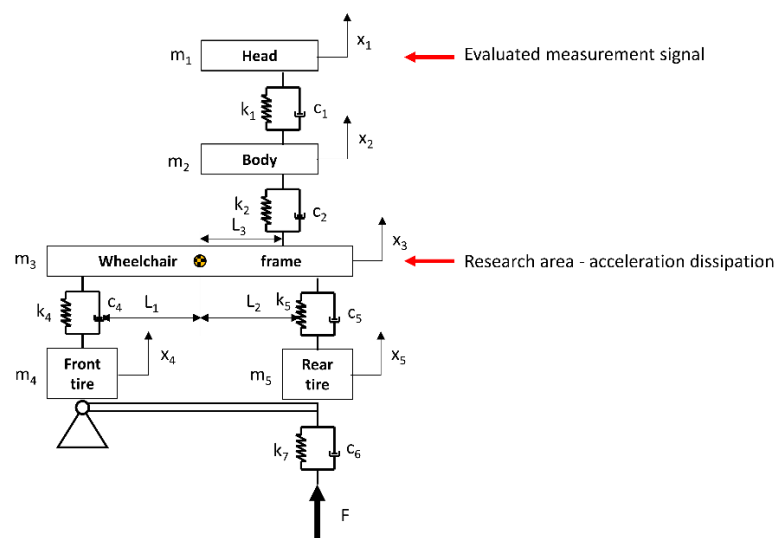


Figure 3. The schematic diagram of the analytical model, taking into account the segment for which the research was conducted, where m_i —mass of the segment, k_i —stiffness constant, c_i —damping constant, L_3 —distance from the chair center to the human center, L_2 —distance from the chair center to the rear side, L_1 —distance from the chair center to the front, x_i —displacement of the segments, F —forcing function.

Based on the above schematic, analytical equations describing the displacements of individual elements of the system (1) can be formulated as follows:

$$\begin{aligned}
 & \begin{bmatrix} m_1 & 0 & 0 & 0 & 0 & 0 \\ 0 & m_2 & 0 & 0 & 0 & 0 \\ 0 & 0 & m_3 & 0 & 0 & 0 \\ 0 & 0 & 0 & \ddot{I} & 0 & 0 \\ 0 & 0 & 0 & 0 & m_4 & 0 \\ 0 & 0 & 0 & 0 & 0 & m_5 \end{bmatrix} \begin{bmatrix} \ddot{x}_1 \\ \ddot{x}_2 \\ \ddot{x}_3 \\ \ddot{\Phi} \\ \ddot{x}_4 \\ \ddot{x}_5 \end{bmatrix} \\
 + & \begin{bmatrix} C_1 & -C_1 & 0 & 0 & 0 & 0 \\ C_1 & C_1 + C_2 & -C_2 & C_1(-L_2 + L_3) & 0 & 0 \\ 0 & -C_2 & C_2 + C_3 + C_4 & C_2(L_2 - L_3) - C_3L_1 + C_4L_2 & -C_3 & -C_4 \\ 0 & -C_2L_3 & C_2L_3 + C_3L_1 + C_4L_2 & C_2L_2 - C_2L_3^2 - C_3L_1^2 + C_4L_2^2 & -C_3L_1 & -C_4L_2 \\ 0 & 0 & -C_4 & C_4L_1 & C_4 + C_6 & 0 \\ 0 & 0 & -C_5 & -C_5L_2 & 0 & C_5 + C_7 \end{bmatrix} \begin{bmatrix} \dot{x}_1 \\ \dot{x}_2 \\ \dot{x}_3 \\ \dot{\Phi} \\ \dot{x}_4 \\ \dot{x}_5 \end{bmatrix} \\
 + & \begin{bmatrix} K_1 & -K_1 & 0 & 0 & 0 & 0 \\ K_1 & K_1 + K_2 & -K_2 & K_1(-L_2 + L_3) & 0 & 0 \\ 0 & -K_2 & K_2 + K_3 + K_4 & K_2(L_2 - L_3) - K_3L_1 + K_4L_2 & -K_3 & -K_4 \\ 0 & -K_2L_3 & K_2L_3 + K_3L_1 + K_4L_2 & K_2L_2 - K_2L_3^2 - K_3L_1^2 + K_4L_2^2 & -K_3L_1 & -K_4L_2 \\ 0 & 0 & -K_4 & K_4L_1 & K_4 + K_6 & 0 \\ 0 & 0 & -K_5 & -K_5L_2 & 0 & K_5 + K_7 \end{bmatrix} \begin{bmatrix} x_1 \\ x_2 \\ x_3 \\ \Phi \\ x_4 \\ x_5 \end{bmatrix} \\
 & = \begin{bmatrix} 0 \\ 0 \\ F \\ F \cdot L_3 \\ 0 \\ 0 \end{bmatrix} \tag{1}
 \end{aligned}$$

2.4. Signal Processing Research Methodology

The research procedure assumed mounting the tested wheelchair in a system generating kinematic excitations (Figure 2) [27]. This system generated a sudden vertical displacement of the rear wheels of the wheelchair to a height of 15 mm in 3 s intervals. This method of generating kinematic excitations is referenced in the works of other researchers using a round rod with a diameter of 3/8" (9.53 mm) to generate vibrations of a similar amplitude and frequency [28]. This interaction resulted in the excitation of vibrations that propagated from the wheelchair's drive wheels to the frame and seat, ultimately reaching the study participant's body. The numerical interpretation of the generated vibrations was expressed as an *R* function of the acceleration time of the accelerometer mounted on the head of a person sitting in a wheelchair. The procedure for processing the measurement signal is shown in Figure 4. According to this algorithm, the value of the *R* resultant acceleration measured with an accelerometer as a function of time was used to analyze vibrations.

Five measurement samples were isolated from the measured *R* acceleration as a function of time course, discarding the extreme values (A1). Then, seven consecutive maximum values (A2) of the *R* resultant acceleration were searched for each isolated sample of cyclically repeating kinematic excitation. On this basis, a set of points representing the time t_n and the amplitude A_n corresponding to this time were defined. Based on this set, the variability of the *R* acceleration amplitude as an *A6* function of time was first analyzed. This analysis determined the average *A* value of the amplitudes (2) from all isolated measurement samples. And this average was represented as a function of the

normalized t_{norm} excitation duration (3). A graphical interpretation of these arithmetic operations below is shown in Figure 5.

$$avg. A_n = \frac{\sum_{i=1}^{i=5} A_{n,i}}{5} \tag{2}$$

$$t_{norm}^n = \frac{\sum_{i=1}^{i=5} (t_{n,i} - t_{n-1,i})}{5} \tag{3}$$

where n —number of the cycle in the analyzed measurement sample of kinematic excitation, i —number of the separated measurement sample, A —amplitude value, t —time value for the performed amplitude observation.

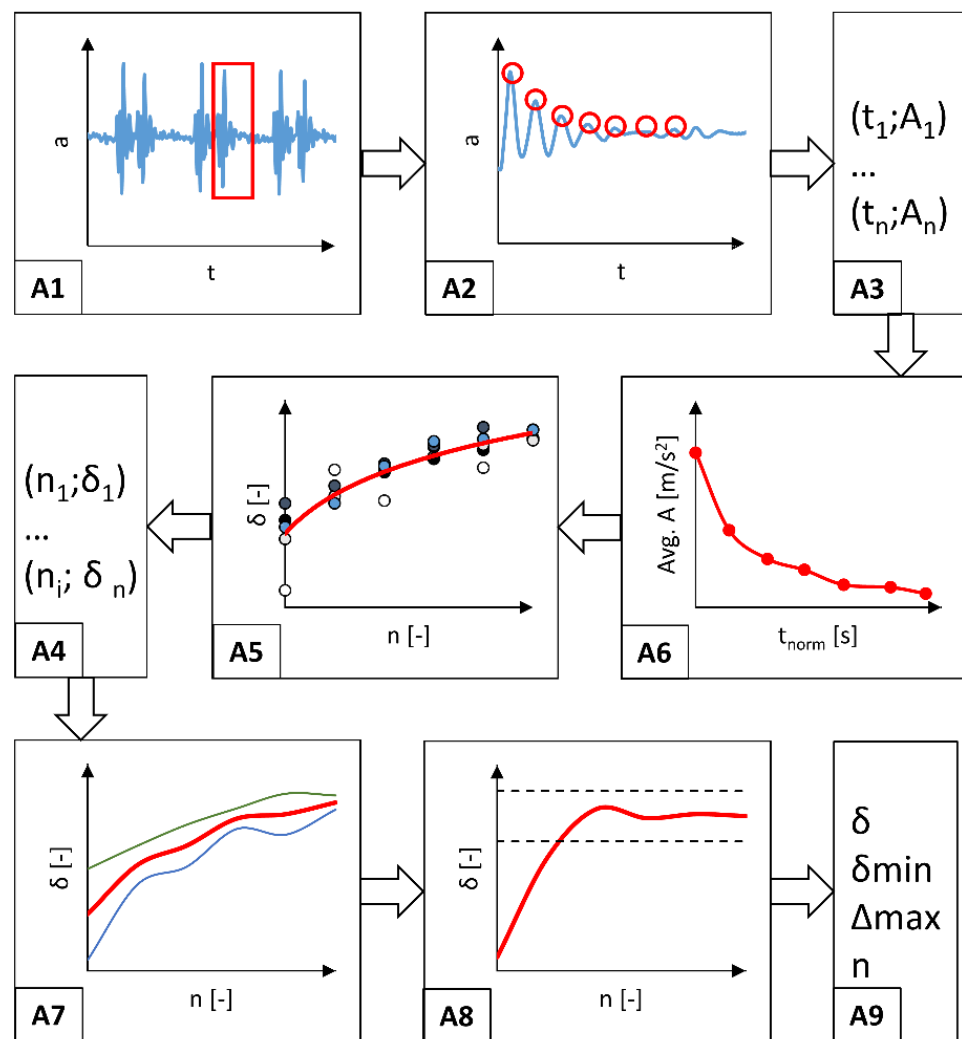


Figure 4. Schematic representation of the algorithm for processing the measurement signal recorded using the accelerometer, where: A1–A9 are steps of the algorithm (description of steps included in the text).

In the next stage of the performed analysis, the value of the δ_n damping decrement (Figure 4(A5)) (4) [29] was calculated for the subsequent A_i amplitudes in relation to the first and maximum amplitude value (Figure 4(A1)) in the cycle selected for analysis from the recorded measurement test.

$$\delta_n = \frac{A_0}{A_{n+1}} ; n = 0, \dots, 6 \tag{4}$$

where δ_n —an n -th value of the damping decrement for the analyzed kinematic excitation cycle, A_1 —a value of the first amplitude of the analyzed kinematic excitation cycle, A_{n+1} —second and subsequent values of the amplitude of the analyzed kinematic excitation cycle.

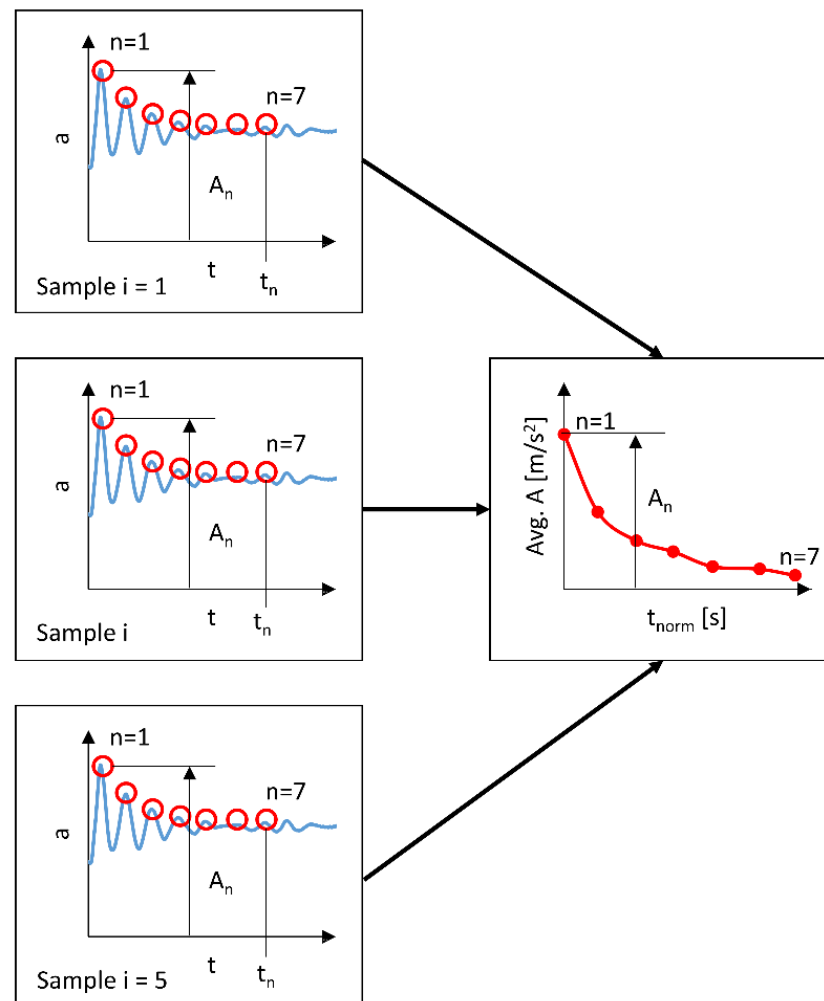


Figure 5. Diagram of extracting amplitudes of head acceleration a from the consistent cycles of kinematic excitation and method of measuring the average value of the average amplitude A .

The determined damping decrement values for five measurement samples representing separate cycles of the measured kinematic excitation (Figure 4(A4)) were then averaged, and the limits of the confidence interval were calculated using the student's t -distribution and the confidence level $p = 0.05$ (Figure 4(A7)). This average value of the damping decrement was used to analyze the amplitudes after reaching the point at which the damping decrement value stabilizes at an equal level. Stabilization of the damping decrement was considered fulfilled if the value of the n th δ_n damping decrement was in the range of $\langle \delta_6 - 0.5\%; \delta_6 + 0.5\% \rangle$ (Figure 5), and when at the same time the value of the measured R acceleration vector was approximately 1 g (approximately 9.81 m/s^2), which is the value that naturally affects the wheelchair at rest in the force field of Earth's gravity. Figure 6 illustrates the stabilization of the damping decrement over a specific range.

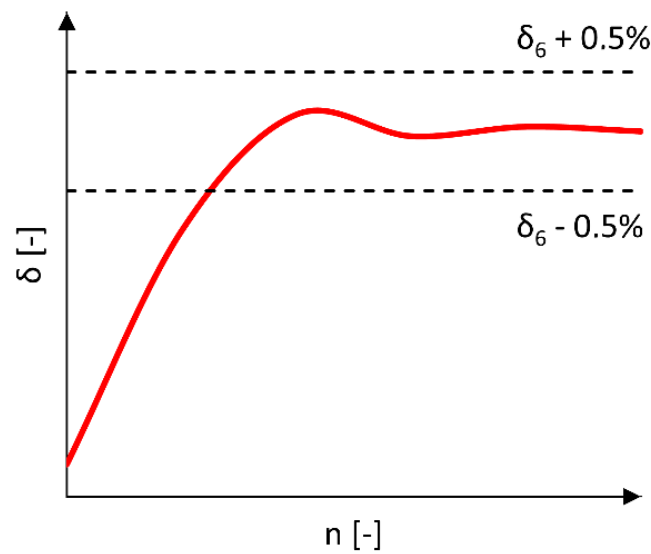


Figure 6. Diagram of the interval used to analyze the stabilization of the δ damping decrement.

3. Results and Discussion

The results of the analysis of vibration amplitude values for the three tested wheelchairs are presented in Figure 7 and Table 2. Upon analyzing the acquired results, it was observed that the value of the first A_1 amplitude of the R vector, occurring after the initiation of kinematic excitation, consistently ranged from 10.85 to 10.95 m/s^2 , regardless of the frame structure of the wheelchair, which constitutes a slight difference of only 0.1 m/s^2 . Additionally, a similar increase in the acceleration value acting on the head was observed in other scientific works using a similar method of generating kinematic excitation [30]. In his research, Philip S. Requejo generated acceleration acting on the user’s head, reaching a maximum of 12 m/s^2 [28]. A slight difference in this value may result from differences in the design features of the excitation generator (steel cylinder on which the wheelchair drive wheel rolled) and design differences of the tested wheelchairs. The importance of the influence of the generator of kinematic excitations type is confirmed by research carried out by Philip S. Requejo, who, in his subsequent studies, generated kinematic excitations during a wheelchair descent from a curb [31]. In this case, the acceleration value increased significantly, reaching values from 1.69 to 1.33 G.

Table 2. Amplitude values for a time interval equal to seven times the vibration period for three compared wheelchair variants: WA—a wheelchair with an aluminum frame, WCBK—a wheelchair with a carbon fiber frame with a standard seat, WCK—a wheelchair with a carbon fiber frame and bucket seat. Where: T —average vibration period with a confidence interval, t_{norm} —normalized value of the duration of the analyzed vibrations, A —vibration amplitude at subsequent amplitudes.

n	T (s)	t_{norm} (s)	WA		T (s)	t_{norm} (s)	WCBK		T (s)	t_{norm} (s)	WCK	
			A (m/s^2)	\pm (m/s^2)			A (m/s^2)	\pm (m/s^2)			A (m/s^2)	\pm (m/s^2)
		0	10.92	0.03		0	10.92	0.12		0	10.85	0.09
1	0.250 ± 0.031	0.218	10.36	0.19	0.250 ± 0.063	0.350	10.18	0.13	0.252 ± 0.057	0.344	10.13	0.05
2		0.468	10.15	0.09		0.648	9.98	0.09		0.628	9.95	0.05
3		0.708	10.07	0.08		0.880	9.88	0.05		0.868	9.90	0.06
4		0.964	9.96	0.03		1.080	9.90	0.03		1.098	9.89	0.04
5		1.268	9.95	0.07		1.298	9.89	0.03		1.286	9.87	0.04
6		1.498	9.90	0.01		1.502	9.89	0.06		1.510	9.87	0.02

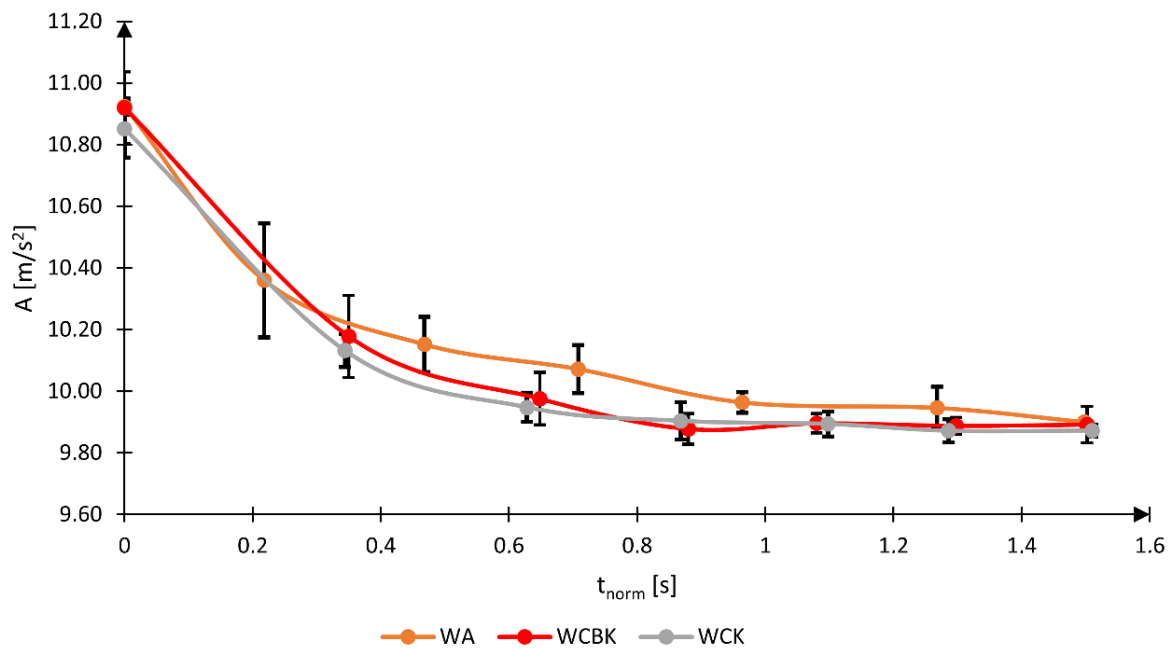


Figure 7. Graph of the change in amplitude as a function of normalized time with the limits of the confidence interval marked for the significance level $p = 0.05$ (WA—a wheelchair with an aluminum frame, WCBK—a wheelchair with a carbon fiber frame with a standard seat, WCK—a wheelchair with a frame made of carbon fiber and with a bucket seat, t_{norm} —normalized value of the duration of the analyzed vibrations, A—vibration amplitude).

The analysis of the A_7 amplitude of the R vector, i.e., the seventh amplitude after the kinematic excitation initiation, showed that regardless of the type of the tested wheelchair, the acceleration acting on the human head reaches a value similar to the acceleration corresponding to a wheelchair at rest located in the Earth's gravitational field. When the A_7 amplitude was reached, the value of the R vector ranged from 9.87 m/s^2 to 9.90 m/s^2 , which is a difference of 0.03 m/s^2 . Additionally, this result is close to the acceleration value due to gravity, proving that the initiated kinematic excitation is damped after a time equal to seven times the T period. In the tested cases, this time was approximately 1.5 s for the average $T = 0.250 \text{ s}$.

The analysis of vibration amplitudes for wheelchairs made of carbon fiber composite (WCBK and WCK) showed that its value in the first oscillations is almost equal despite the difference in the seat system design. The analysis of the acceleration oscillations showed that in the case of a wheelchair with an aluminum alloy frame (WA) for the time interval from 0.4 to 1.2 s , the amplitude value is higher than for carbon fiber wheelchairs (WCBK and WCK). The peak value of the difference in the value of the vibration R vector in these amplitudes is 0.75 m/s^2 , which occurs in the time interval from 0.6 to 0.8 s . This observation is confirmed by the work describing the impact of the construction material and construction features on the transmission and damping of vibrations [32–35].

The impact of long-term vibrations and sudden accelerations on the human body is unfavorable due to the risk of health deterioration [36,37]. Therefore, a beneficial operating property of a wheelchair is the shortest possible time needed to reduce the acceleration acting on the human body to a level close to 1 g . Consequently, further research analyzed the value of the damping δ decrement and observed when its value stabilized over time [38]. The constant value of δ as a function of time indicates that the analyzed value of the A_i acceleration amplitudes has stabilized (Figure 8). The adopted research methodology translated into a reduction in the acceleration acting on the head to approximately 1 g . The analysis of the damping decrement of the tested wheelchairs was performed based on five separate time courses of the R vector. Each separated signal began until the kinematic

excitation acted on the tested system and lasted seven times the T period, allowing to observe the n number of deflections of the A_1 amplitude, equal to $n = 7$.

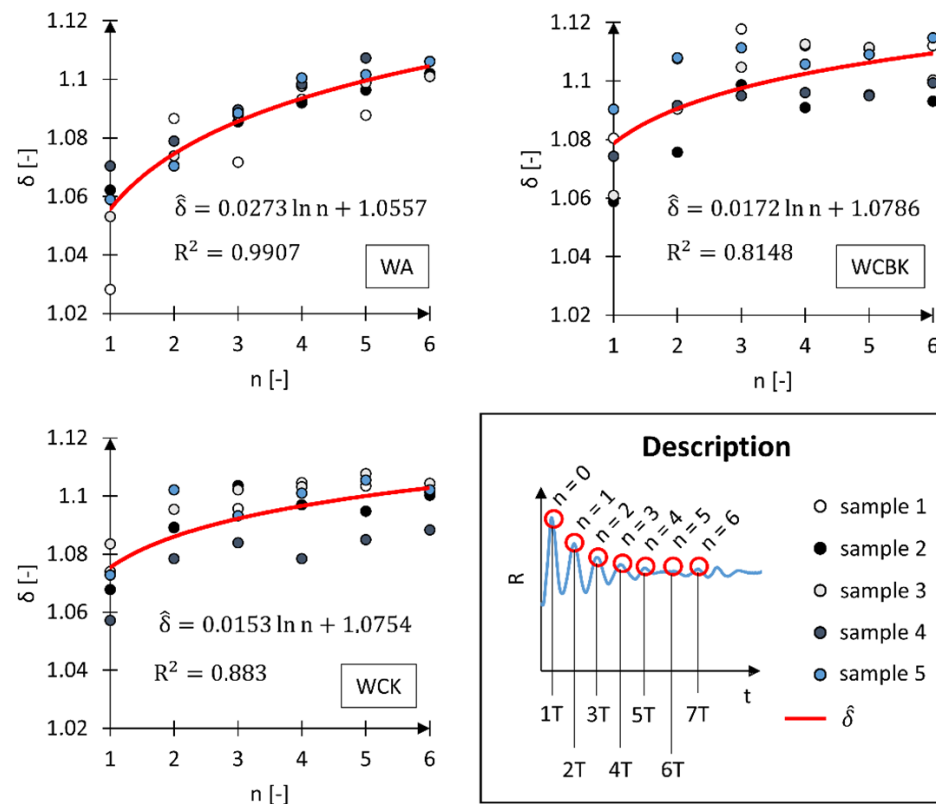


Figure 8. Dependence of the damping decrement δ relative to the first oscillation ($n = 0$) for a wheelchair with an aluminum alloy frame (WA), an active wheelchair with a carbon fiber frame with a standard seat (WCBK), and an active wheelchair with a carbon fiber frame with bucket seat (WCK). δ —damping decrement, $\hat{\delta}$ —function characterizing the variability of the average value of the damping decrement, n —oscillation number, T —period, R^2 —coefficient of determination.

The analysis results of the δ damping decrement indicate that in the case of the WA wheelchair, the initial value of the damping decrement is much smaller than in the case of the WCBK and WCK wheelchairs. The value of δ for the oscillation corresponding to $n = 1$ is in the ranges: from 1.028 to 1.070 for the WA wheelchair, from 1.059 to 1.090 for the WCBK wheelchair, and from 1.057 to 1.083 for the WCK wheelchair. By analyzing the function that describes the variability of the average damping decrement δ , we found that in the case of wheelchairs made of carbon fiber composite (WCBK and WCK), the curve showing the change in damping decrement flattens much earlier than in the case of the WA wheelchair. Therefore, another analysis was performed, this time checking the variability of the average value of the δ_{avg} damping decrement as a function of the number of the analyzed n oscillations (Figure 9).

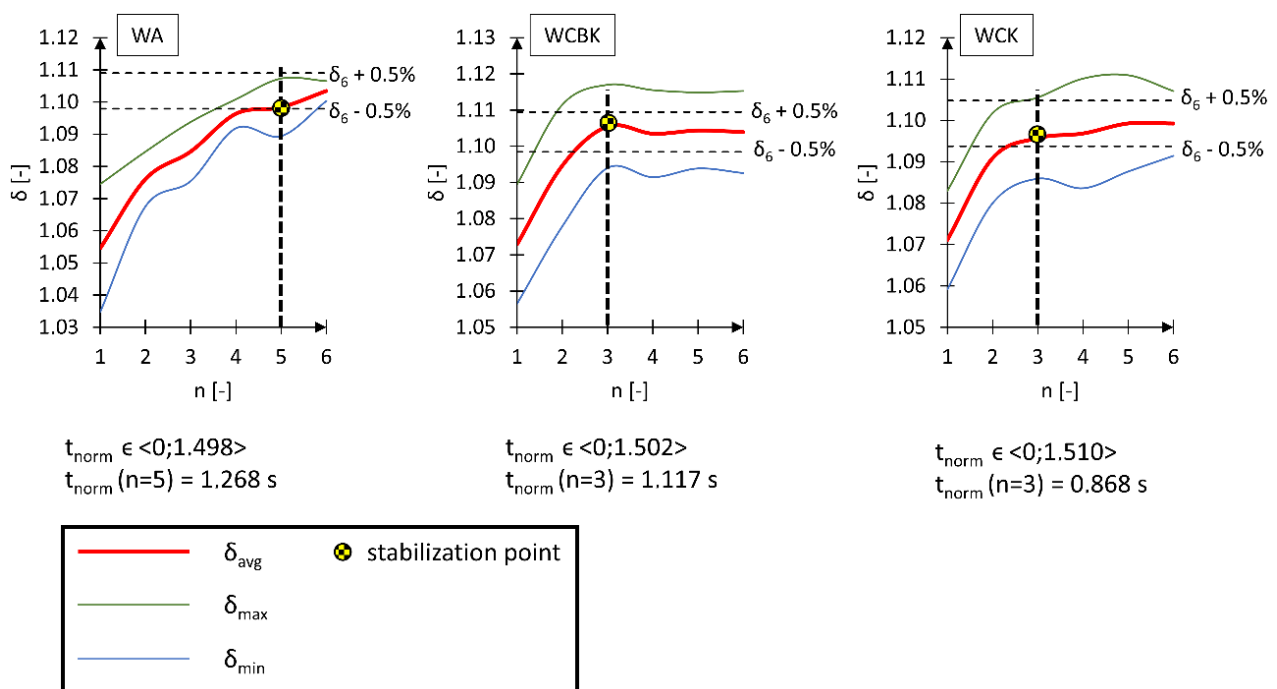


Figure 9. Graphs of the average value of the δ_{avg} damping decrement variability for an active wheelchair with an aluminum frame (WA), an active wheelchair with a carbon fiber frame with a standard seat (WCBK), and an active wheelchair with a carbon fiber frame with a bucket seat (WCK). δ_{avg} —average damping decrement, δ_{max} —maximum damping decrement, δ_{min} —minimum damping decrement, t_{norm} —normalized time of the observed damping phenomenon of the kinematic excitation, n —number of the observed oscillation of the kinematic deflection.

In the δ_{avg} analysis performed following the research methodology, it was assumed that the value of the damping decrement of subsequent amplitudes (from A_1 to A_n) is constant if it falls within the range of $\delta(n = 6) \pm 0.5\%$. This assumption means that the ratio of the first measured amplitude to the n -th consecutive amplitude is approximately equal (5).

$$\frac{A_0}{A_n} \approx \frac{A_0}{A_{n+1}} \approx \frac{A_0}{A_{n+2}} \leftrightarrow \sigma_n \approx \sigma_{n+1} \approx \sigma_{n+2} \quad (5)$$

The average δ_{avg} damping decrement analysis confirmed previous observations stating that WCBK and WCK wheelchairs dampen the initiated kinematic excitation more quickly. This phenomenon results from using a new material for this type of construction, i.e., carbon fiber composite, which is confirmed in the literature [39]. For the WA wheelchair, stabilization of δ_{avg} occurred after the t_{norm} time of 1.268 s with a total duration of the kinematic excitation of 1.498 s. This constituted approximately 85% of the entire duration of the kinematic excitation. In the case of the WCBK and WCK wheelchairs, the stabilization of δ_{avg} occurred after the t_{norm} time, which was 1.117 s and 0.868 s, respectively. This constituted 74% of the total duration of the kinematic excitation for the WCBK wheelchair and 58% for the WCK. Based on the direct measurement of vibration acceleration, it is possible to indirectly determine, for instance, the mechanical energy transferred to the human body. Similar acceleration calculations allowing the determination of mechanical and energy parameters are carried out in many fields of science [40–43].

4. Conclusions

The conducted research has shown that the use of modern materials to construct a wheelchair frame requires an interdisciplinary approach to the design process, which also takes into account factors such as the ability to dampen vibrations. The use of materials or design solutions that effectively reduce vibrations translates directly into the comfort of

using the wheelchair and reduces the risk to the health of its user. The kinematic excitation used in the study resulted in a linear acceleration acting on the human head ranging from 10.85 to 10.92 m/s². Using the same method of generating kinematic excitation for all tested wheelchairs, similar values of the vibration amplitude measured on the wheelchair user's head in the zero cycle (A_0) were obtained. Therefore, it can be concluded that the frame structure and the material from which the tested wheelchairs were made do not reduce the value of the R acceleration vector.

Based on the performed tests, it was also found that the material and geometry of the tested wheelchairs only influenced the time of dissipation of mechanical energy caused by kinematic excitation. During the WA wheelchair test, the initiated kinematic excitation decreases to the value of 9.81 m/s², corresponding to the acceleration due to gravity after performing five analyzed oscillations. However, in the case of WCBK and WCK wheelchairs, the kinematic excitation was reduced to 9.81 m/s² after just three analyzed oscillations. It should be noted that seven consecutive oscillations were used in the analyses, the first of which, marked with the number 0, was the reference value for calculating the damping decrement. The results confirm that modern construction materials can be an alternative to additional wheelchair suspension modules that dampen vibrations caused by kinematic excitations.

Reducing the duration of dynamic overloads affecting the human body is a significant problem that translates directly into the health of the wheelchair user. The research showed that one of the possible solutions to this problem is using modern engineering materials, such as carbon fiber-reinforced composites. The performed damping decrement analysis showed an increase of 10% in the rate of dissipation of mechanical energy generating vibrations of the human body for the WCBK wheelchair compared to the structure of a wheelchair with an aluminum alloy frame (WA) and an increase of 32% in the rate of mechanical energy dissipation for WCK wheelchair compared to the structure of a wheelchair with an aluminum frame (WA). WCBK and WCK wheelchairs, despite better results compared to the WA wheelchair, show a significant difference in results. These wheelchairs had the same structure of the supporting frame and drive system elements but differed in the seat arrangement. Therefore, further research should assess how individual elements of the wheelchair structure made of carbon fiber affect the kinematic excitation operation time reduction.

Author Contributions: Conceptualization, B.W. and Ł.W.; methodology, B.W., Ł.W., J.A., T.S., M.P., Ł.P. and M.S.; software, B.W.; validation, B.W.; formal analysis, B.W., Ł.W., J.A., T.S., M.P., Ł.P. and M.S.; investigation, B.W. and T.S.; resources, B.W., M.P. and Ł.P.; data curation, B.W.; writing—original draft preparation, B.W., Ł.W. and M.S.; writing—review and editing, B.W., Ł.W. and M.S.; visualization, B.W.; supervision, B.W.; project administration, B.W.; funding acquisition, T.S. and B.W. All authors have read and agreed to the published version of the manuscript.

Funding: Funding for publication of the article is provided from subvention of the Ministry of Science and Higher Education, category: Other scientific activities.

Institutional Review Board Statement: Not applicable.

Informed Consent Statement: Not applicable.

Data Availability Statement: Data are contained within the article.

Acknowledgments: The authors thank Cosmotech for delivering wheelchairs for research and substantive support.

Conflicts of Interest: Author Michał Padjasek and Łukasz Padjasek were employed by the company Cosmotech LLC, Szyby Rycerskie 22k St., 41-909 Bytom, Poland. The remaining authors declare that the research was conducted in the absence of any commercial or financial relationships that could be construed as a potential conflict of interest.

References

1. Branowski, B.; Pohl, P.; Rychlik, M.; Zablocki, M. Integral Model of the Area of Reaches and Forces of a Disabled Person with Dysfunction of Lower Limbs as a Tool in Virtual Assessment of Manipulation Possibilities in Selected Work Environments. In Proceedings of the Universal Access in Human-Computer Interaction, Orlando, FL, USA, 9–14 July 2011; Stephanidis, C., Ed.; Users Diversity. Springer: Berlin/Heidelberg, Germany, 2011; pp. 12–21.
2. Ahasan, R.; Campbell, D.; Salmoni, A.; Lewko, J. Ergonomics of Living Environment for the People with Special Needs. *J. Physiol. Anthropol. Appl. Human Sci.* **2001**, *20*, 175–185. [[CrossRef](#)]
3. Sydor, M.; Pop, J.; Jasińska, A.; Zablocki, M. Anthro-Mechanical Cradles: A Multidisciplinary Review. *Int. J. Environ. Res. Public Health* **2022**, *19*, 15759. [[CrossRef](#)]
4. Wieczorek, B. The Wheelchair Propulsion Wheel Rotation Angle Function Symmetry in the Propelling Phase: Motion Capture Research and a Mathematical Model. *Symmetry* **2022**, *14*, 576. [[CrossRef](#)]
5. Warguła, Ł.; Marciniak, A. The Symmetry of the Muscle Tension Signal in the Upper Limbs When Propelling a Wheelchair and Innovative Control Systems for Propulsion System Gear Ratio or Propulsion Torque: A Pilot Study. *Symmetry* **2022**, *14*, 1002. [[CrossRef](#)]
6. Maeda, S.; Futatsuka, M.; Yonesaki, J.; Ikeda, M. Relationship between Questionnaire Survey Results of Vibration Complaints of Wheelchair Users and Vibration Transmissibility of Manual Wheelchair. *Environ. Health Prev. Med.* **2003**, *8*, 82–89. [[CrossRef](#)]
7. Herrera-Saray, P.; Peláez-Ballestas, I.; Ramos-Lira, L.; Sánchez-Monroy, D.; Burgos-Vargas, R. Usage Problems and Social Barriers Faced by Persons With a Wheelchair and Other Aids. Qualitative Study From the Ergonomics Perspective in Persons Disabled by Rheumatoid Arthritis and Other Conditions. *Reumatol. Clínica Engl. Ed.* **2013**, *9*, 24–30. [[CrossRef](#)]
8. Blach Rossen, C.; Sørensen, B.; Würtz Jochumsen, B.; Wind, G. Everyday Life for Users of Electric Wheelchairs—A Qualitative Interview Study. *Disabil. Rehabil. Assist. Technol.* **2012**, *7*, 399–407. [[CrossRef](#)]
9. Krantz, O.; Egard, H. Use of Active Wheelchairs in Everyday Life: Experiences among Experienced Users of Active Ultra Lightweight Rigid Frame Wheelchairs. *Disabil. Rehabil. Assist. Technol.* **2017**, *12*, 65–72. [[CrossRef](#)] [[PubMed](#)]
10. Hong, S.-W.; Patrangenaru, V.; Singhose, W.; Sprigle, S. Identification of Human-Generated Forces on Wheelchairs during Total-Body Extensor Thrusts. *Clin. Biomech.* **2006**, *21*, 790–798. [[CrossRef](#)] [[PubMed](#)]
11. Sprigle, S.; Linden, M. Accelerations Experienced by Wheelchair Users with Spinalcord Injury in a Moving Van. *Technol. Disabil.* **1996**, *5*, 81–91. [[CrossRef](#)]
12. Sitnik, L.J.; Magdziak-Tokłowicz, M.; Wróbel, R.; Kardasz, P. Vehicle Vibration in Human Health. *J. KONES* **2013**, *20*, 411–418. [[CrossRef](#)]
13. Smith, S.D. Characterizing the Effects of Airborne Vibration on Human Body Vibration Response. *Aviat. Space Environ. Med.* **2002**, *73*, 36–45.
14. Graaf, B.D.; Van Weperen, W. The Retention of Balance: An Exploratory Study into the Limits of Acceleration the Human Body Can Withstand without Losing Equilibrium. *Hum. Factors* **1997**, *39*, 111–118. [[CrossRef](#)] [[PubMed](#)]
15. Wieczorek, B.; Kaczmarzyk, P.; Warguła, Ł.; Giedrowicz, M.; Bąk, D.; Gierz, Ł.; Stambolov, G.; Kostov, B. Research on the Distribution of Axial Excitation of Positive Pressure Ventilators in the Aspect of Stability Safety of the Load-Bearing Frame. *Adv. Sci. Technol. Res. J.* **2023**, *18*, 142–154. [[CrossRef](#)] [[PubMed](#)]
16. Wolf, E.J.; Cooper, M.S.R.A.; DiGiovine, C.P.; Boninger, M.L.; Guo, S. Using the Absorbed Power Method to Evaluate Effectiveness of Vibration Absorption of Selected Seat Cushions during Manual Wheelchair Propulsion. *Med. Eng. Phys.* **2004**, *26*, 799–806. [[CrossRef](#)] [[PubMed](#)]
17. Garcia-Mendez, Y.; Pearlman, J.L.; Cooper, R.A.; Boninger, M.L. GDynamic Stiffness and Transmissibility of Commercially Available Wheelchair Cushions Using a Laboratory Test Method. *J. Rehabil. Res. Dev.* **2012**, *49*, 7. [[CrossRef](#)] [[PubMed](#)]
18. Chwalik-Pilszyk, G.; Dziechciowski, Z.; Kromka-Szydek, M.; Koziń, M. Experimental Study of the Influence of Using Polyurethane Cushion to Reduce Vibration Received by a Wheelchair User. *Acta Bioeng. Biomech.* **2023**, *25*, 137–149. [[CrossRef](#)]
19. Kwarcia, A.M.; Cooper, R.A.; Ammer, W.A.; Fitzgerald, S.G.; Boninger, M.L.; Cooper, R. Fatigue Testing of Selected Suspension Manual Wheelchairs Using ANSI/RESNA Standards. *Arch. Phys. Med. Rehabil.* **2005**, *86*, 123–129. [[CrossRef](#)] [[PubMed](#)]
20. Giwnewer, U.; Rubin, G.; Friedman, A.; Rozen, N. User Assessment of a Novel Suspension for a Wheelchair—A Prospective, Randomized, Double Blind Trial. *Geriatr. Orthop. Surg. Rehabil.* **2020**, *11*, 2151459320983268. [[CrossRef](#)] [[PubMed](#)]
21. Dzierżek, K.; Buczyłowski, A.; Kamiński, K.; Rólkowski, P.; Tylman, I.; Rećko, M.; Ostaszewski, M.; Turycz, P. Design and Static Tests of an All-Terrain Suspension System for Electric Wheelchair. In Proceedings of the 2018 International Conference BIOMDLORE, Białystok, Poland, 28–30 June 2018; pp. 1–5.
22. Hostens, I.; Papaioannou, Y.; Spaepen, A.; Ramon, H. A Study of Vibration Characteristics on a Luxury Wheelchair and a New Prototype Wheelchair. *J. Sound Vib.* **2003**, *266*, 443–452. [[CrossRef](#)]
23. Cooper, R.A. A Perspective on the Ultralight Wheelchair Revolution. *Technol. Disabil.* **1996**, *5*, 383–392. [[CrossRef](#)]
24. Gebrosky, B.; Grindle, G.; Cooper, R.; Cooper, R. Comparison of Carbon Fibre and Aluminium Materials in the Construction of Ultralight Wheelchairs. *Disabil. Rehabil. Assist. Technol.* **2020**, *15*, 432–441. [[CrossRef](#)] [[PubMed](#)]
25. Worobey, L.A.; Bernstein, J.; Ott, J.; Berner, T.; Black, J.; Cabarle, M.; Roesler, T.; Scarborough, S.; Betz, K. RESNA Position on the Application of Ultralight Manual Wheelchairs. *Assist. Technol.* **2023**, *0*, 1–18. [[CrossRef](#)] [[PubMed](#)]
26. PN-EN ISO 5349-1:2004; Measurement and Determination of Human Exposure to Vibrations Transmitted by the Upper Limbs—Part 1: General Requirements. ISO: Geneva, Switzerland, 2004.

27. Wieczorek, B.; Warguła, Ł. Problems of Dynamometer Construction for Wheelchairs and Simulation of Push Motion. *MATEC Web Conf.* **2019**, *254*, 01006. [[CrossRef](#)]
28. Requejo, P.S. Effect of Rear Suspension and Speed on Seat Forces and Head Accelerations Experienced by Manual Wheelchair Riders with Spinal Cord Injury. *J. Rehabil. Res. Dev.* **2008**, *45*, 985–996. [[CrossRef](#)]
29. Hans, S.; Ibraim, E.; Pernot, S.; Boutin, C.; Lamarque, C.-H. Damping Identification in Multi-Degree-of-Freedom System via a Wavelet-Logarithmic Decrement—Part 2: Study of a Civil Engineering Building. *J. Sound Vib.* **2000**, *235*, 375–403. [[CrossRef](#)]
30. Lariviere, O.; Chadefaux, D.; Sauret, C.; Thoreux, P. Vibration Transmission during Manual Wheelchair Propulsion: A Systematic Review. *Vibration* **2021**, *4*, 444–481. [[CrossRef](#)]
31. Requejo, P.; Maneekobkunwong, S.; McNitt-Gray, J.; Adkins, R.; Waters, R. Influence of Hand-Rim Wheelchairs with Rear Suspension on Seat Forces and Head Acceleration during Curb Descent Landings. *J. Rehabil. Med.* **2009**, *41*, 459–466. [[CrossRef](#)]
32. Chénier, F.; Aissaoui, R. Effect of Wheelchair Frame Material on Users' Mechanical Work and Transmitted Vibration. *BioMed Res. Int.* **2014**, *2014*, e609369. [[CrossRef](#)]
33. Yilmazcoban, I.K.; Mimaroglu, A. Frontal Impact Absorbing Systems in Wheelchairs like Sheet Metal Hood in Vehicles. *Thin-Walled Struct.* **2012**, *59*, 20–26. [[CrossRef](#)]
34. DiGiovine, C.P.; Cooper, R.A.; Fitzgerald, S.G.; Boninger, M.L.; Wolf, E.J. Songfeng Guo Whole-Body Vibration during Manual Wheelchair Propulsion with Selected Seat Cushions and Back Supports. *IEEE Trans. Neural Syst. Rehabil. Eng.* **2003**, *11*, 311–322. [[CrossRef](#)]
35. Cooper, R.A.; Wolf, E.; Fitzgerald, S.G.; Boninger, M.L.; Ulerich, R.; Ammer, W.A. Seat and Footrest Shocks and Vibrations in Manual Wheelchairs with and without Suspension. *Arch. Phys. Med. Rehabil.* **2003**, *84*, 96–102. [[CrossRef](#)] [[PubMed](#)]
36. Rantaharju, T.; Mansfield, N.J.; Ala-Hiio, J.M.; Gunston, T.P. Predicting the Health Risks Related to Whole-Body Vibration and Shock: A Comparison of Alternative Assessment Methods for High-Acceleration Events in Vehicles. *Ergonomics* **2015**, *58*, 1071–1087. [[CrossRef](#)] [[PubMed](#)]
37. Eiband, A.M. *Human Tolerance to Rapidly Applied Accelerations: A Summary of the Literature*; NASA: Washington, DC, USA, 1959.
38. Little, J.A.; Mann, B.P. Optimizing Logarithmic Decrement Damping Estimation through Uncertainty Propagation. *J. Sound Vib.* **2019**, *457*, 368–376. [[CrossRef](#)]
39. Jeon, E.-B.; Ahn, S.; Lee, I.-G.; Koh, H.-I.; Park, J.; Kim, H.-S. Investigation of Mechanical/Dynamic Properties of Carbon Fiber Reinforced Polymer Concrete for Low Noise Railway Slab. *Compos. Struct.* **2015**, *134*, 27–35. [[CrossRef](#)]
40. Szpica, D. Validation of Indirect Methods Used in the Operational Assessment of LPG Vapor Phase Pulse Injectors. *Measurement* **2018**, *118*, 253–261. [[CrossRef](#)]
41. Świć, A.; Gola, A.; Orynycz, O.; Tucki, K.; Matijošius, J. Technological Methods for Controlling the Elastic-Deformable State in Turning and Grinding Shafts of Low Stiffness. *Materials* **2022**, *15*, 5265. [[CrossRef](#)]
42. Žvirblis, T.; Vainorius, D.; Matijošius, J.; Kilikevičienė, K.; Rimkus, A.; Bereczky, Á.; Lukács, K.; Kilikevičius, A. Engine Vibration Data Increases Prognosis Accuracy on Emission Loads: A Novel Statistical Regressions Algorithm Approach for Vibration Analysis in Time Domain. *Symmetry* **2021**, *13*, 1234. [[CrossRef](#)]
43. Sawczuk, W.; Ulbrich, D.; Kowalczyk, J.; Merkiusz-Guranowska, A. Evaluation of Wear of Disc Brake Friction Linings and the Variability of the Friction Coefficient on the Basis of Vibroacoustic Signals. *Sensors* **2021**, *21*, 5927. [[CrossRef](#)]

Disclaimer/Publisher's Note: The statements, opinions and data contained in all publications are solely those of the individual author(s) and contributor(s) and not of MDPI and/or the editor(s). MDPI and/or the editor(s) disclaim responsibility for any injury to people or property resulting from any ideas, methods, instructions or products referred to in the content.